THE JOURNAL OF PHYSICAL CHEMISTRY C LETTERS

2008, *112,* 13336–13341
Published on Web 08/13/2008

Examining Förster Energy Transfer for Semiconductor Nanocrystalline Quantum Dot Donors and Acceptors

Carles Curutchet,[†] Alberto Franceschetti,[‡] Alex Zunger,[‡] and Gregory D. Scholes*,[†]

Department of Chemistry, 80 St. George Street, Institute for Optical Sciences, and Centre for Quantum Information and Quantum Control, University of Toronto, Toronto, Ontario M5S 3H6 Canada, and National Renewable Energy Laboratory, Golden, Colorado 80401

Received: June 27, 2008; Revised Manuscript Received: July 23, 2008

Excitation energy transfer involving semiconductor quantum dots (QDs) has received increased attention in recent years because their properties, such as high photostability and size-tunable optical properties, have made QDs attractive as Förster resonant energy transfer (FRET) probes or sensors. An intriguing question in FRET studies involving QDs has been whether the dipole approximation, commonly used to predict the electronic coupling, is sufficiently accurate. Accurate estimates of electronic couplings between two 3.9 nm CdSe QDs and between a QD and a chlorophyll molecule are reported. These calculations are based on transition densities obtained from atomistic semiempirical calculations and time-dependent density functional theory for the QD and the chlorophyll, respectively. In contrast to the case of donor−acceptor molecules, where the dipole approximation breaks down at length scales comparable to the molecular dimensions, we find that the dipole approximation works surprisingly well when donor and/or acceptor is a spherical QD, even at contact donor−acceptor separations. Our conclusions provide support for the use of QDs as FRET probes for accurate distance measurements.

The special properties of semiconductor nanocrystalline quantum dots (QD), such as high photostability, size-tunable optical properties, and the possibility to functionalize their surfaces with particular ligands have inspired a breadth of research,[1−6] including building ordered assemblies of QDs, studies of biological sensing,[7−9] quantum computation,[10−12] and the proposal of solar energy conversion devices.[13−16] A feature of the multidot assemblies studied in that context is the observation and use of electronic energy transfer (EET) process, where an electronically excited donor system (atom, molecule, or nanocrystal) transfers its excitation energy to a nearby acceptor in a nonradiative way.[17] EET has been demonstrated between QDs,[18−22] between organic polymers and QDs,[23−25] and between QDs and molecular probes in the context of fluorophore tagging in biological systems.[7−9,26−28] Theoretical studies have also been reported.[10−12,29,30] Recently, it has been suggested that QDs can be used as probes in long-range Förster resonance energy transfer (FRET) distance measurements up to 13 nm.[31] The potential use of QDs as FRET probes, however, will only turn into a practical application if EET between QDs and molecular dyes can be appropriately described by the Förster mechanism.

Although EET between weakly coupled molecular systems has been the focus of substantial research and is well understood,[17] EET between QDs donor−acceptor pairs or between QDs and molecules is not well understood, and still fundamental questions remain unclear. For example, in EET involving molecular pairs[17] at length-scales comparable to the dimensions of the molecules, the Förster mechanism with its underlying dipole approximation breaks down, and a more accurate representation is needed to obtain reliable estimates of the coupling.[32−36] Considering that in EET involving QDs the distances are typically in the same range as the size of the QDs, that is, from 1 to 8 nm, how good is the dipole approximation for these systems? The problem can be described by comparing the general, transition density-based expression for EET with the popular point-dipole (Förster) expression.

The general, weak coupling formula for predicting the rate of EET between a single electronic state of a donor D and an acceptor A is given by

$$k_{\mathrm{EET}} = \frac{2\pi}{\hbar} |s V_s|^2 J \tag{1}$$

where J is the normalized overlap between donor emission and acceptor absorption spectra,[17] s is the solvent screening factor, approximated as $1/n^2$, where n is the refractive index of the medium, and V_s is the electronic coupling between D and A transition densities. This electronic coupling is given by the two-electron integral that represents de-excitation of the donor and concomitant electronic excitation of the acceptor. The interaction is Coulombic, representing coupling between transition densities connecting the ground state and excited state for the donor and acceptor. The electronic coupling, obtained from transition densities is hence

$$V_s^{(3D)} = \int \frac{\rho_{ge}^{D}(\mathbf{r}_1)\rho_{eg}^{A}(\mathbf{r}_2)}{|\mathbf{r}_1 - \mathbf{r}_2|} d\mathbf{r}_1 d\mathbf{r}_2 \tag{2}$$

Given the transition densities $\rho_{ge}^{D}(\mathrm{r})$ and $\rho_{eg}^{A}(\mathrm{r})$, it is possible to compute the "exact" EET rate (in the weak coupling limit)

* To whom correspondence should be addressed. E-mail: gscholes@chem.utoronto.ca.
[†] University of Toronto.
[‡] National Renewable Energy Laboratory.

10.1021/jp805682m CCC: $40.75

from eqs 1 and 2, assuming that the D and A electron densities do not overlap and do not distort each other.

Traditionally, the transition densities are expanded as a multipole series, and then eq 2 would be evaluated as the interaction between the multipoles corresponding to D and A[37]

$$V_s^{(\text{multipole})} = V_{\text{dip-dip}} + V_{\text{dip-quad}} + V_{\text{quad-dip}} + V_{\text{dip-oct}} + V_{\text{oct-dip}} + V_{\text{quad-quad}} + \ldots \quad (3)$$

The coupling $V_s^{(\text{multipole})}$ given by eq 3 reproduces the exact result of eq 2 provided that an untruncated multipole expansion is used and that the multipoles are calculated exactly from the same transition densities, that is, $\mu_{\text{eg},\alpha}^{\text{QD}} = \int r_\alpha \rho_{\text{eg}}^{\text{QD}}(\mathbf{r})d\mathbf{r}$. In the classic Förster theory,[38] the coupling is obtained by truncating this expansion to the first term, which is an interaction between transition dipole moments. This so-called point-dipole approximation gives the characteristic R^{-6} decay of the rates

$$V_s^{(\text{multipole})} \approx V_{\text{dip-dip}} = \frac{\kappa \mu_D^T \mu_A^T}{R^3} \quad (4)$$

where μ_D^T/μ_A^T are transition dipole moments of D and A separated by a distance R, and the orientation factor, κ, is defined in terms of the angles between transition moments and the donor−acceptor vector.[17] In the case of QDs, the relevant transition moments follow selection rules for circularly polarized light[6,39] so care needs to be taken when determining κ.[12] Often an orientational average is taken, such that $\kappa^2 \rightarrow 2/3$ is used in the rate expression.

Here we compare the EET rate obtained from the unapproximated, 3D formula of eq 2, with the multipole expansion of eq 3 and the classic point-dipole approximation of eq 4. We consider (i) two identical 3.9 nm diameter CdSe wurtzite QDs, and (ii) a CdSe QD and a nearby chlorophyll-*a* molecule (Chl). The density matrices of eq 2 for CdSe are obtained from atomistic pseudopotential calculations in a plane wave basis, whereas the density matrices for chlorophyll are obtained from time-dependent density functional calculations in a Gaussian basis. We find that in contrast to what is typically observed in EET involving two molecules, the point-dipole approximation gives an excellent estimate of electronic couplings for the three different orientations between the donor and the acceptor we consider, both for the QD−Chl and QD−QD systems, even at close-contact separations. This latter result is in agreement with a recent study of QD−QD pairs that employed semiempirical calculations based on the tight-binding Hamiltonian.[29]

We explain the accuracy of the dipole approximation qualitatively on the basis of the quasi-spherical symmetry of the negatively and positively charged clouds that form the QD transition densities. These create an electrostatic potential that effectively behaves as the potential originated by a positive charge and a negative charge located at the center of the QD and separated by ~7 Å. Our conclusions thus provide support for the use of QDs as FRET probes for long-range distance measurements.

The electronic couplings $V_s^{(3D)}$ were computed by evaluating the integral in eq 2 using a discretization of the transition densities into finite volume elements over a 3D grid for the donor and the acceptor, and the elements of the cubes are subsequently interacted via the coulomb potential, as described elsewhere.[32,40] The accuracy of this integration, often known as the transition density cube method (TDC), depends only on the quality of the discretization procedure adopted, which can be controlled by using sufficiently fine grids.[32] For CdSe dots, we discretized the transition density on a noncubic grid of finite elements with volume ~0.6 bohr^3 to calculate the electronic couplings, whereas for the Chl molecule we used the transition density finely discretized in finite elements with volume ~0.04 bohr^3. The accuracy of calculating $V_s^{(3D)}$ from the actual quantum-mechanical 3D transition densities thus depends essentially only on the level of sophistication used to derive the quantum mechanical transition densities themselves, as described next.

The transition density for 3.9 nm diameter wurtzite CdSe QDs was obtained from atomistic single-particle wave functions calculated using the semiempirical pseudopotential method.[41] In this approach, we solve the Schrödinger equation

$$\left[-\frac{\hbar^2}{2m}\nabla^2 + V_{\text{LOC}}(\boldsymbol{r}) + \hat{V}_{\text{NL}} + \hat{V}_{\text{SO}}\right]\psi_i(\boldsymbol{r},\sigma) = \varepsilon_i \psi_i(\boldsymbol{r},\sigma) \quad (5)$$

where m is the bare electron mass, $V_{\text{LOC}}(\mathbf{r})$is the local pseudopotential, $\hat{V}_{\text{NL}}$ is the nonlocal pseudopotential operator, and $\hat{V}_{\text{SO}}$ is the spin−orbit operator. The local pseudopotential is given by the superposition of screened atomic potentials υ_n centered at the atomic positions$\mathbf{R}_n$:

$$V_{\text{LOC}}(\boldsymbol{r}) = \sum\nolimits_n \upsilon_n(\boldsymbol{r} - \boldsymbol{R}_n) \quad (6)$$

The atomic potentials υ_n, as well as the nonlocal pseudopotential $\hat{V}_{\text{NL}}$ and the spin−orbit operator $\hat{V}_{\text{SO}}$, were optimized by fitting calculations to experimental bulk transition energies, effective masses, and deformation potentials, and ab initio calculated bulk wave functions.[41] Equation 5 is solved by expanding the wave functions $\psi_i(r,\sigma)$ in a plane-wave basis set and using the folded-spectrum method[42] to selectively calculate the band-edge states. The pseudopotential method fully includes intervalley coupling and intraband coupling. The transition density of the isolated QD was calculated as

$$\rho_{\text{eg}}^{\text{QD}}(\boldsymbol{r}) = \sum\nolimits_\sigma \psi_v^*(\boldsymbol{r},\sigma)\psi_c(\boldsymbol{r},\sigma) \quad (7)$$

where ψ_v and ψ_c denote the single-particle valence (v) and conduction (c) wave functions. We thus neglect excitonic effects, such as electron−hole Coulomb attraction and exchange coupling, on the transition density. Electron−hole Coulomb attraction leads to a shift of the exciton energy compared to the single-particle band gap, but because of strong quantum confinement, Coulomb interactions cause only minor changes to the electron and hole wave functions and thus to the transition density. Electron−hole exchange interactions lead to fine-structure splitting (dark/bright splitting) of the exciton ground state. Since the dark/bright splitting of the CdSe QD considered here is only ~5 meV,[43] the bright exciton states are thermally populated at room temperature, so eq 7 is a good approximation to the transition density.

Regarding the chlorophyll molecule, we consider the transition density of the Q_y lowest-lying bright state, which was obtained from time-dependent density functional theory (TD-DFT) calculations using the hybrid B3LYP exchange-correlation functional and the 6-31+G(d) basis set for the isolated Chl. Prior geometry optimization was performed at the B3LYP/6-31G level. Both geometry optimization and excited-states of Chl were calculated with the Gaussian 03 package.[44] We obtained a vertical excitation energy of 2.09 eV and a transition dipole moment of 5.45 Debye.

Distance-dependent coupling profiles were calculated by adopting fixed relative orientations of the donor and the acceptor and then systematically varying their center-to-center separation. In Figure 1, we show a schematic representation of the orientations considered for the QD−QD and the QD−Chl pairs indicating the relevant angles that have been varied to generate

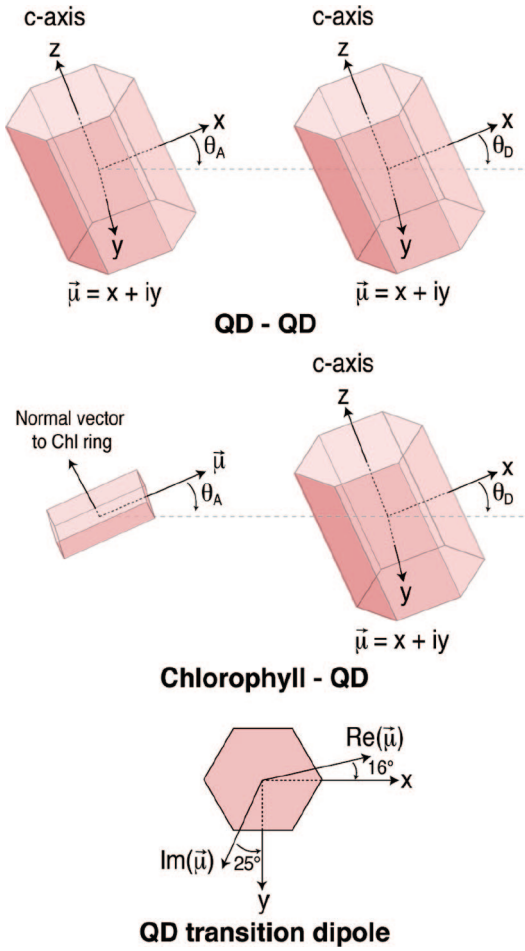

Figure 1. Schematic representation of the relative orientation of the QD−QD and QD−Chl pairs studied in this work. The angles θ_D and θ_A have been varied in both pairs to generate different orientations. Selection rules for circularly polarized light give rise to a complex transition moment for the QD, with real and imaginary components approximately along the *x* and *y* axis. At the bottom we show the actual components of the complex transition dipole obtained in our calculations, which slightly deviate from the crystallographic axis. We have used the direction defined by the predicted Re($\vec{\mu}$) as the actual *x* axis used to define the relative orientations.

the different orientations. In particular, we have considered (i) a face-to-face (FF) orientation ($\theta_D = -\pi/2$ and $\theta_A = -\pi/2$), (ii) a head-to-tail (HT) orientation ($\theta_D = 0$, $\theta_A = 0$), and (iii) a diagonal-like (DL) orientation ($\theta_D = 3\pi/4$ and $\theta_A = 3\pi/4$). For the QD−QD pair, electronic couplings were estimated at center-to-center separations in the range 42.5−105 Å using 2.5 Å steps between the closest points (<55 Å) and 5 Å steps for the rest. For the QD−Chl pair, separations in the range 22.5−55 Å (FF orientation) and 27.5−55 Å (HT and DL orientations) were considered, and the coupling was again computed every 2.5 Å for the closest points (<40 Å) and every 5 Å for the rest.

Figure 2 shows the transition densities corresponding to the FF orientation of the QD−QD and QD−Chl pairs, where their marked dipolar character can be clearly seen. Here we note that, as indicated in Figure 1, selection rules for circularly polarized light give rise to a complex dipole transition moment (and transition density) for the QD with real and imaginary components approximately along the *x* and *y* axes, respectively. In our discussion of the results, we consider the absolute square of the corresponding complex couplings obtained, as this is the relevant ingredient for the prediction of EET rates.

Figures 3 and 4 show the distance-dependent profiles of squared couplings V_s corresponding to the QD−QD and

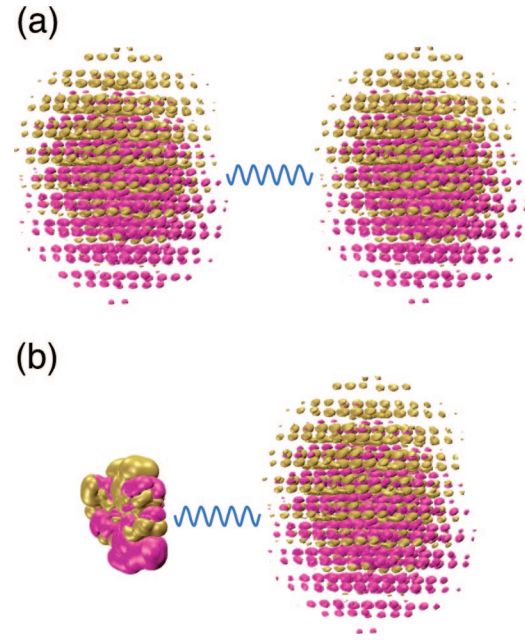

Figure 2. Graphical representation of the transition densities of the systems studied in this work. (a) Two CdSe QDs oriented face-to-face (FF). (b) Chl and CdSe QD oriented face-to-face (FF). Note that the real part of the complex transition density is displayed for the QDs. Images created with VMD.[49]

QD−Chl pairs, respectively, as obtained in the FF and HT orientations both from the point-dipole approximation, eq 4, and the full 3D expression integrated numerically within the TDC method, eq 2. (Figures corresponding to the DL orientations are included as Supporting Information.) In the point-dipole approximation, we used the point dipoles evaluated from the same quantum mechanical orbitals used to evaluate $V_s^{(3D)}$ calculated according to

$$\mu_{eg,\alpha}^{QD} = \int r_\alpha \rho_{eg}^{QD}(\mathbf{r})\mathrm{d}\mathbf{r} \tag{8}$$

where the index α denotes the *x*, *y*, and *z* components of the vector, and the integral was solved numerically over the discretized transition density. Figures 3 and 4 show that the agreement between the 3D expression and the point-dipole approximation for the QD−QD pair is excellent along the whole distance profiles and for all the orientations considered. Even at QD−QD quasi-contact separations (42.5 Å), in all cases deviations smaller than 3% are found to arise as a consequence of the point-dipole approximation in the estimated rates.

For the Chl−QD pair, the disagreement between the exact 3D expression and the point-dipole approximation is slightly increased at close separations. However, the effect in the estimated rates is in all cases smaller than 25%. In particular, we found deviations equal to 17, 9, and 24% for the closest distances considered with FF, HT, and DL orientations, respectively, which correspond to deviations in the coupling of 8, 5, and 11%. Moreover, at distances >35 Å, which corresponds to approximately ∼15 Å between the center of the Chl and the QD surface, the error in the point-dipole approximation on the rates becomes smaller than 10%.

To gain a better understanding on the origin of the differences between the full 3D coupling and the point-dipole expression eq 4, we also computed the coupling from a multipole expansion of the interaction including dipole, quadrupole, and octapole terms.[37] As for the dipole transition moment, quadrupole and octapole transition moments were obtained from the corre-

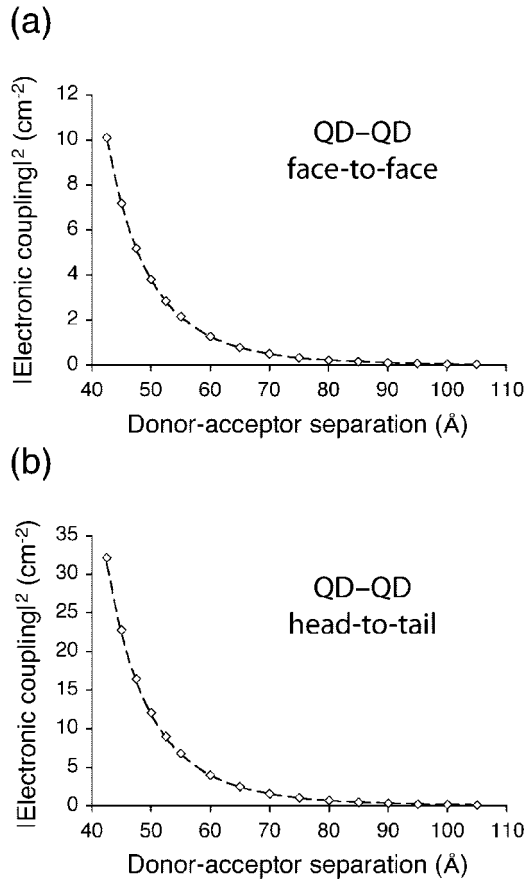

Figure 3. Squared electronic couplings predicted by the full 3D expression (diamonds) and by the point dipole approximation (dashed lines) between two 3.9 nm CdSe QDs as a function of their center-to-center separation. (a) Face-to-face (FF) orientation. (b) Head-to-tail (HT) orientation.

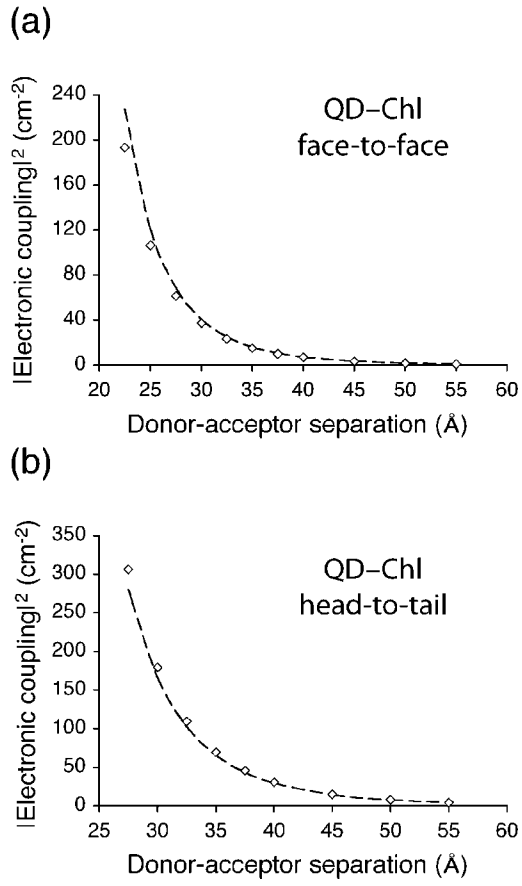

Figure 4. Squared electronic couplings predicted by the full 3D expression (diamonds) and by the point dipole approximation (dashed lines) between a chlorophyll molecule and a 3.9 nm CdSe QD as a function of their center-to-center separation. (a) Face-to-face (FF) orientation. (b) Head-to-tail (HT) orientation.

sponding transition densities. In Tables 1 and 2, we report the electronic couplings obtained from the point-dipole, exact 3D, and the multipole expansion expressions for the QD−QD and QD−Chl pairs, respectively. Such couplings are obtained at the closest center-to-center separations considered in the FF and HT orientations, that is, almost at contact separations. Here, we note that for larger separations higher multipole contributions are expected to be less important due to their more pronounced distance decay compared to the dipole−dipole term. For the QD−QD system, we find that the consideration of quadrupole and octapole terms in the coupling leads to negligible changes less than 3% in the predicted rates, in accord with the excellent agreement found between the exact 3D and the point-dipole estimates. For the QD−Chl pair, the effect of such higher multipoles is more important. In this case, the inclusion of quadrupole and octapole terms leads to changes of ∼15% in the multipolar expansion couplings compared to the point-dipole values, which lead to a better agreement with respect to the predictions of the exact 3D result. In particular, couplings involving the quadrupole transition moment are small because of the symmetry of the transition, and the largest contribution of higher multipoles is found to arise as a consequence of the octapole of the Chl molecule, rather than that of the QD.

An explanation for the unexpected close agreement between the exact 3D couplings and those obtained considering simple point dipoles can be surmised from electrostatic considerations. From the graphical representation of the transition densities shown in Figure 2, it is apparent that the transition density of the QD is built up from two quasi-spherical clouds with opposite sign. It is a well-known result in classical electrostatics that the external potential generated by a spherically symmetric charge distribution can be described as the potential generated by a point charge located at its center and carrying the same amount of charge. Thus, the potential generated by the QD transition density can be approximated as the sum of the potentials generated by two point charges located at the centers of such oppositely signed clouds. For the QD we consider, such centers of charge are separated by ∼7 Å. Thus we can effectively describe the QD transition density as a transition dipole defined by two charges separated by such distance, which is clearly smaller than the center-to-center separations accessible to donors and acceptors. From this point of view, then, it is not surprising that the point-dipole approximation is able to accurately predict the coupling over the complete range of center-to-center separations that we test for the QD−QD pair, as these are in all cases much larger than 7 Å. On the other hand, the small deviation found at close separations for the QD−Chl system can be ascribed to deficiencies in the description of the Chl transition density by the point-dipole, as in this case the transition dipole is averaged on the size of Chl (∼10−15 Å), which is only slightly smaller than the closest distances considered for this pair. This is confirmed by the substantially larger effect of including quadrupole and octapole transition moments of Chl in the multipole expansion analysis compared to those of the QD.

Our results for the QD−QD pair are in accord with a recent study by Allan and Delerue,[29] in which electronic couplings between two InAs QDs, obtained using a semiempirical atom-

TABLE 1: Electronic Couplings, EET Rates, and EET Times between Two 3.9 nm CdSe QDs Calculated by Using the Full 3D, the Point-Dipole, and the Multipole Expansion Expression Including Dipole, Quadrupole, and Octupole Terms

	Re(V)/cm^{-1}	Im(V)/cm^{-1}	$\|V\|^2$/cm^{-2}	k_{EET}/ns^{-1}[a]	τ_{EET}/ns[a]
		FF[b], R = 22.5 Å			
$V_s^{(3D)}$	−1.742	−2.660	10.1	1.20	0.84
$V_{dip\text{-}dip}$	−1.738	−2.659	10.1	1.19	0.84
$V_s^{(multipole)}$[c]	−1.750	−2.695	10.3	1.22	0.82
$V_{dip\text{-}quad}$	0.003	−0.011			
$V_{quad\text{-}dip}$	0.003	−0.011			
$V_{dip\text{-}oct}$	−0.009	−0.007			
$V_{oct\text{-}dip}$	−0.009	−0.007			
$V_{quad\text{-}quad}$	0.000	0.000			
		HT[b], R = 27.5 Å			
$V_s^{(3D)}$	−1.783	5.383	32.2	3.81	0.26
$V_{dip\text{-}dip}$	−1.779	5.317	31.4	3.72	0.27
$V_s^{(multipole)}$[c]	−1.799	5.452	33.0	3.90	0.26
$V_{dip\text{-}quad}$	0.015	0.018			
$V_{quad\text{-}dip}$	0.015	0.018			
$V_{dip\text{-}oct}$	0.005	0.050			
$V_{oct\text{-}dip}$	0.005	0.050			
$V_{quad\text{-}quad}$	0.000	−0.001			

[a] EET times and rates obtained considering a spectral overlap of 10^{-4} cm as obtained in ref 12. [b] Face-to-face (FF) and head-to-tail (HT) orientations; see text for details. [c] Multipole expansion coupling,[37] $V_s^{(multipole)} = V_{dip\text{-}dip} + V_{dip\text{-}quad} + V_{quad\text{-}dip} + V_{dip\text{-}oct} + V_{oct\text{-}dip} + V_{quad\text{-}quad}$.

TABLE 2: Electronic Couplings, EET Rates and EET Times Estimated for the 3.9 nm CdSe QD− Chl Pair by Using the Full 3D, the Point-Dipole, and the Multipole Expansion Expression Including Dipole, Quadrupole, and Octupole Terms

	Re(V)/cm^{-1}	Im(V)/cm^{-1}	$\|V\|^2$/cm^{-2}	k_{EET}/ns^{-1}[a]	τ_{EET}/ns[a]
		FF[b], R = 22.5 Å			
$V_s^{(3D)}$	9.841	−9.837	193.6	22.91	0.044
$V_{dip\text{-}dip}$	10.696	−10.605	226.9	26.85	0.037
$V_s^{(multipole)}$[c]	10.216	−10.043	205.2	24.28	0.041
$V_{dip\text{-}quad}$	0.137	−0.036			
$V_{quad\text{-}dip}$	0.156	−0.040			
$V_{dip\text{-}oct}$	−0.011	−0.044			
$V_{oct\text{-}dip}$	−0.769	0.687			
$V_{quad\text{-}quad}$	0.007	−0.005			
		HT[b], R = 27.5 Å			
$V_s^{(3D)}$	−12.443	12.323	306.7	36.30	0.028
$V_{dip\text{-}dip}$	−11.834	11.820	279.8	33.11	0.030
$V_s^{(multipole)}$[c]	−12.499	13.426	336.5	39.81	0.025
$V_{dip\text{-}quad}$	0.017	−0.038			
$V_{quad\text{-}dip}$	0.100	−0.249			
$V_{dip\text{-}oct}$	−0.186	0.239			
$V_{oct\text{-}dip}$	−0.592	0.599			
$V_{quad\text{-}quad}$	−0.004	0.003			

[a] EET times and rates estimated considering a standard value for the spectral overlap of 10^{-4} cm. [b] Face-to-face (FF) and head-to-tail (HT) orientations; see text for details. [c] Multipole expansion coupling,[37] $V_s^{(multipole)} = V_{dip\text{-}dip} + V_{dip\text{-}quad} + V_{quad\text{-}dip} + V_{dip\text{-}oct} + V_{oct\text{-}dip} + V_{quad\text{-}quad}$. $V_{quad\text{-}dip}/V_{oct\text{-}dip}$ refer to higher multipoles of Chl and $V_{dip\text{-}quad}/V_{dip\text{-}oct}$ of the QD.

istic approach based on the tight binding Hamiltonian, were shown to be appropriately described by the dipole−dipole approximation. On the other hand, a recent study of Baer and Rabani[30] analyzed the role of higher multipoles in energy transfer involving two CdSe QDs in the context of the effective mass approximation. The key point of that work is to explore how other electronic states of the acceptor QD can play a role in EET. Transfers between the lowest (dipole-allowed) bright states, as those considered in our work, were discussed as usual in terms of dipole−dipole interactions. However, the possibility that dipole forbidden (weakly allowed) transitions may act as energy acceptors was evaluated. In such cases the first term in eq 3 is zero, but the dipole−quadrupole term can mediate EET. In very recent work, calculations of electronic couplings based on the TDC approach have been reported for CdSe nanorods.[45] That work provides a striking contrast to our results, showing that the dipole approximation is quite unsuccessful for these nanocrystals.

We note that in the present study we have not considered the effect of the surrounding environment on the EET coupling, which is accounted for in Förster theory through the simple $s = 1/n^2$ screening factor in eq 1. A better approximation of s is obtained if one considers two transition dipoles with each one inserted in spherical cavities inside the medium, which leads to a screening $s = (9n^2)/(2n^2 + 1)^2$.[29,30] Recently, a more rigorous approach in which the solute is treated at a full quantum-mechanical level and the solvent response is obtained solving the Poisson equation for molecular-shaped cavities inside the dielectric medium has shown how the shape of interacting chromophores strongly modulates the screening factor, especially at close donor−acceptor separations where the system shares a common cavity inside the medium.[36,46] However, for QDs the $s = (9n^2)/(2n^2 + 1)^2$ factor is expected to be a significantly better approximation than for molecules for two important reasons. One reason is that their shapes are in general closer to a sphere, and the second reason is that the external potential produced by their transition density, which triggers the solvent response that in turn screens the interaction, can be effectively described as that generated by a dipole source, as discussed above.

We also note that in the two recent studies discussed above[29,30] the dielectric properties of the QDs are also considered when discussing the screening of EET couplings. However, in the context of FRET measurements the experimentalist should note that such an effect is already included in the measured transition dipoles, which are further corrected by a local field factor that depends on the dielectric properties of the surrounding medium. Similarly, if one uses quantum-mechanical methods that appropriately account for the microscopic interactions in the system Hamiltonian, as commonly done in the context of molecular systems (e.g., our density functional theory calculations on Chl), there is no need to introduce the macroscopic dielectric constant of the molecule in the calculation of EET couplings.

In our analysis, we use transition densities calculated for the isolated molecule and QD. However, the surrounding environment can lead to changes in the transition densities, and consequently, introduce an additional indirect effect on the coupling. While this effect is expected to be small for QDs,[47] the surrounding environment[36] or the presence of nearby QDs[48] can potentially lead to significant changes in the transition density of the Chl molecule.

Finally, we estimate the order of magnitude expected for the EET times, which correspond to k_{EET}^{-1} as given by eq 1. Such times are estimated on the basis of the calculated couplings and an experimental spectral overlap integral derived for CdSe QDs by properly averaging over realizations of inhomogenous broadening, $\langle J \rangle \approx 10^{-4}$ cm.[12] We find that EET times at close separations are of the order of nanoseconds (see Supporting Information for complete data), which is in agreement with experiments reported on assemblies of CdSe QDs, where

0.7−1.9 ns EET times were observed,[20] as well as with the theoretical predictions of Baer and Rabani.[30] We also roughly estimate the order of magnitude of accessible EET rates expected for a CdSe QD/dye pair by considering a standard value of the spectral overlap of 10^{-4} cm and the electronic couplings obtained for the QD−Chl system. In this case, we estimate EET rates ranging from several tens to hundreds of picoseconds at close separations. Again, such orders of magnitude are in reasonable agreement with experiments reported on similar CdSe QD−phthalocyanine conjugates in which EET times in the range 24−769 ps were measured.[28]

We conclude that there is an unexpected excellent agreement between the dipole approximation and accurate estimates of the coupling obtained from quantum-mechanically derived transition densities for dipole-allowed transitions. That is in contrast to what is typically observed for molecular probes, and constitutes a previously unidentified advantage that supports the use of QDs in FRET studies.

Acknowledgment. The Natural Sciences and Engineering Research Council of Canada is gratefully acknowledged for support of this research. G.D.S. acknowledges the support of an E.W.R. Steacie Memorial Fellowship. Work at NREL was supported by Office of Science, Basic Energy Sciences, Materials Sciences, and Engineering, under Contract No. DE-AC36-99GO10337 to NREL. We thank Mr. Yaser Khan for valuable discussion on this work.

Supporting Information Available: Complete tables of electronic couplings for the QD−QD and QD−Chl pairs, components of the transition dipole moment of the QD, and graphical representation of squared coupling profiles for the DL orientation. This material is available free of charge via the Internet at http://pubs.acs.org.

References and Notes

(1) Alivisatos, A. P. *Science* **1996**, *271*, 933.
(2) Weller, H. *Angew. Chem., Int. Ed.* **1993**, *32*, 41.
(3) Rogach, A. L.; Eychmuller, A.; Hickey, S. G.; Kershaw, S. V. *Small* **2007**, *3*, 536.
(4) Nozik, A. J. *Chem. Phys. Lett.* **2008**, *457*, 3.
(5) Klimov, V. I. *Annu. Rev. Phys. Chem.* **2007**, *58*, 635.
(6) Scholes, G. D. *Adv. Funct. Mater.* **2008**, *18*, 1157.
(7) Patolsky, F.; Gill, R.; Weizmann, Y.; Mokari, T.; Banin, U.; Willner, I. *J. Am. Chem. Soc.* **2003**, *125*, 13918.
(8) Clapp, A. R.; Medintz, I. L.; Mattoussi, H. *ChemPhysChem.* **2006**, *7*, 47.
(9) Medintz, I. L.; Clapp, A. R.; Mattoussi, H.; Goldman, E. R.; Fisher, B.; Mauro, J. M. *Nat. Mater.* **2003**, *2*, 630.
(10) Govorov, A. O. *Phys. Rev. B* **2003**, *68*, 075315.
(11) Govorov, A. O. *Phys. Rev. B* **2005**, *71*, 155323.
(12) Scholes, G. D.; Andrews, D. L. *Phys. Rev. B* **2005**, *72*, 125331.
(13) Huynh, W. U.; Dittmer, J. J.; Alivisatos, A. P. *Science* **2002**, *295*, 2425.
(14) Timmerman, D.; Izeddin, I.; Stallinga, P.; Yassievich, I. N.; Gregorkiewicz, T. *Nat. Photon.* **2008**, *2*, 105.
(15) Johnston, K. W.; Pattantyus-Abraham, A. G.; Clifford, J. P.; Myrskog, S. H.; MacNeil, D. D.; Levina, L.; Sargent, E. H. *Appl. Phys. Lett.* **2008**, *92*, 151115.
(16) Law, M.; Luther, J. M.; Song, O.; Hughes, B. K.; Perkins, C. L.; Nozik, A. J. *J. Am. Chem. Soc.* **2008**, *130*, 5974.
(17) Scholes, G. D. *Annu. Rev. Phys. Chem.* **2003**, *54*, 57.
(18) Kagan, C. R.; Murray, C. B.; Nirmal, M.; Bawendi, M. G. *Phys. Rev. Lett.* **1996**, *76*, 1517.
(19) Kagan, C. R.; Murray, C. B.; Bawendi, M. G. *Phys. Rev. B* **1996**, *54*, 8633.
(20) Crooker, S. A.; Hollingsworth, J. A.; Tretiak, S.; Klimov, V. I. *Phys. Rev. Lett.* **2002**, *89*, 186802.
(21) Franzl, T.; Shavel, A.; Rogach, A. L.; Gaponik, N.; Klar, T. A.; Eychmuller, A.; Feldmann, J. *Small* **2005**, *1*, 392.
(22) Bose, R.; McMillan, J. F.; Gao, J.; Rickey, K. M.; Chen, C. J.; Talapin, D. V.; Murray, C. B.; Wong, C. W. *Nano Lett.* **2008**, *8*, 2006.
(23) Anni, M.; Manna, L.; Cingolani, R.; Valerini, D.; Creti, A.; Lomascolo, M. *Appl. Phys. Lett.* **2004**, *85*, 4169.
(24) Kaufmann, S.; Stoferle, T.; Moll, N.; Mahrt, R. F.; Scherf, U.; Tsami, A.; Talapin, D. V.; Murray, C. B. *Appl. Phys. Lett.* **2007**, *90*, 071108.
(25) Wang, M.; Kumar, S.; Lee, A.; Felorzabihi, N.; Shen, L.; Zhao, F.; Froimwicz, P.; Scholes, G. D.; Winnik, M. A. *J. Am. Chem. Soc.* **2008**, *130*, 9481.
(26) Clapp, A. R.; Medintz, I. L.; Mauro, J. M.; Fisher, B. R.; Bawendi, M. G.; Mattoussi, H. *J. Am. Chem. Soc.* **2004**, *126*, 301.
(27) Dayal, S.; Lou, Y. B.; Samia, A. C. S.; Berlin, J. C.; Kenney, M. E.; Burda, C. *J. Am. Chem. Soc.* **2006**, *128*, 13974.
(28) Dayal, S.; Burda, C. *J. Am. Chem. Soc.* **2007**, *129*, 7977.
(29) Allan, G.; Delerue, C. *Phys. Rev. B* **2007**, *75*, 195311.
(30) Baer, R.; Rabani, E. *J. Chem. Phys.* **2008**, *128*, 184710.
(31) Lu, H.; Schops, O.; Woggon, U.; Niemeyer, C. M. *J. Am. Chem. Soc.* **2008**, *130*, 4815.
(32) Krueger, B. P.; Scholes, G. D.; Fleming, G. R. *J. Phys. Chem. B* **1998**, *102*, 5378.
(33) Beljonne, D.; Pourtois, G.; Silva, C.; Hennebicq, E.; Herz, L. M.; Friend, R. H.; Scholes, G. D.; Setayesh, S.; Mullen, K.; Bredas, J. L. *Proc. Natl. Acad. Sci. U.S.A.* **2002**, *99*, 10982.
(34) Wong, K. F.; Bagchi, B.; Rossky, P. J. *J. Phys. Chem. A* **2004**, *108*, 5752.
(35) Frahmcke, J. S.; Walla, P. J. *Chem. Phys. Lett.* **2006**, *430*, 397.
(36) Curutchet, C.; Scholes, G. D.; Mennucci, B.; Cammi, R. *J. Phys. Chem. B* **2007**, *111*, 13253.
(37) Scholes, G. D.; Andrews, D. L. *J. Chem. Phys.* **1997**, *107*, 5374.
(38) Forster, T. *Ann. Phys.* **1948**, *2*, 55.
(39) Efros, A. L.; Rosen, M.; Kuno, M.; Nirmal, M.; Norris, D. J.; Bawendi, M. *Phys. Rev. B* **1996**, *54*, 4843.
(40) Scholes, G. D.; Fleming, G. R. *Adv. Chem. Phys.* **2005**, *132*, 57.
(41) Wang, L.-W.; Zunger, A. *Phys. Rev. B* **1995**, *51*, 17398.
(42) Wang, L. W.; Zunger, A. *J. Chem. Phys.* **1994**, *100*, 2394.
(43) Franceschetti, A.; Fu, H.; Wang, L. W.; Zunger, A. *Phys. Rev. B* **1999**, *60*, 1819.
(44) Frisch, M. J. ; Trucks, G. W.; Schlegel, H. B.; Scuseria, G. E.; Robb, M. A.; Cheeseman, J. R.; Montgomery, J., J. A.; Vreven, T.; Kudin, K. N.; Burant, J. C.; Millam, J. M.; Iyengar, S. S.; Tomasi, J.; Barone, V.; Mennucci, B.; Cossi, M.; Scalmani, G.; Rega, N.; Petersson, G. A.; Nakatsuji, H.; Hada, M.; Ehara, M.; Toyota, K.; Fukuda, R.; Hasegawa, J.; Ishida, M.; Nakajima, T.; Honda, Y.; Kitao, O.; Nakai, H.; Klene, M.; Li, X.; Knox, J. E.; Hratchian, H. P.; Cross, J. B.; Bakken, V.; Adamo, C.; Jaramillo, J.; Gomperts, R.; Stratmann, R. E.; Yazyev, O.; Austin, A. J.; Cammi, R.; Pomelli, C.; Ochterski, J. W.; Ayala, P. Y.; Morokuma, K.; Voth, G. A.; Salvador, P.; Dannenberg, J. J.; Zakrzewski, V. G.; Dapprich, S.; Daniels, A. D.; Strain, M. C.; Farkas, O.; Malick, D. K.; Rabuck, A. D.; Raghavachari, K.; Foresman, J. B.; Ortiz, J. V.; Cui, Q.; Baboul, A. G.; Clifford, S.; Cioslowski, J.; Stefanov, B. B.; Liu, G.; Liashenko, A.; Piskorz, P.; Komaromi, I.; Martin, R. L.; Fox, D. J.; Keith, T.; Al-Laham, M. A.; Peng, C. Y.; Nanayakkara, A.; Challacombe, M.; Gill, P. M. W.; Johnson, B.; Chen, W.; Wong, M. W.; Gonzalez, C.; Pople, J. A. *Gaussian 03*, revision B.03; Gaussian, Inc.: Wallingford, CT, 2004.
(45) Schrier, J.; Wang, L.-W. *J. Phys. Chem. C* **2008**, ASAP.
(46) Scholes, G. D.; Curutchet, C.; Mennucci, B.; Cammi, R.; Tomasi, J. *J. Phys. Chem. B* **2007**, *111*, 6978.
(47) Rabani, E.; Hetenyi, B.; Berne, B. J.; Brus, L. E. *J. Chem. Phys.* **1999**, *110*, 5355.
(48) Curutchet, C.; Cammi, R.; Mennucci, B.; Corni, S. *J. Chem. Phys.* **2006**, *125*, 054710.
(49) Humphrey, W.; Dalke, A.; Schulten, K. *J. Mol. Graph.* **1996**, *14*, 33.

JP805682M